Ecotoxicology and Environmental Safety 184 (2019) 109623

Contents lists available at ScienceDirect

Ecotoxicology and Environmental Safety

journal homepage: www.elsevier.com/locate/ecoenv

# Localization, ligand environment, bioavailability and toxicity of mercury in *Boletus* spp. and *Scutiger pes-caprae* mushrooms

Anja Kavčič[a,1], Klemen Mikuš[b,1], Marta Debeljak[c], Johannes Teun van Elteren[c], Iztok Arčon[d,e], Alojz Kodre[d,f], Peter Kump[d], Andreas Germanos Karydas[g], Alessandro Migliori[h], Mateusz Czyzycki[i,j], Katarina Vogel-Mikuš[a,d,*]

[a] University of Ljubljana, Biotechnical Faculty, Department of Biology, Jamnikarjeva 101, SI-1000, Ljubljana, Slovenia
[b] Biotechnical Educational Centre Ljubljana, Cesta V Mestni Log 47, SI-1000, Ljubljana, Slovenia
[c] National Institute of Chemistry, Hajdrihova 19, SI-1000, Ljubljana, Slovenia
[d] Jozef Stefan Institute, Jamova 39, SI-1000, Ljubljana, Slovenia
[e] University of Nova Gorica, Vipavska 13, SI-5000, Nova Gorica, Slovenia
[f] University of Ljubljana, Faculty for Mathematics and Physics, Jadranska 19, SI-1000, Ljubljana, Slovenia
[g] Institute of Nuclear and Particle Physics, National Centre for Scientific Research 'Demokritos', Patr. Grigoriou E' & 27 Neapoleos St, 153 41, Agia Paraskevi, Greece
[h] Nuclear Science and Instrumentation Laboratory, International Atomic Energy Agency (IAEA) Laboratories, A-2444, Seibersdorf, Austria
[i] Karlsruhe Institute of Technology, Institute for Photon Science and Synchrotron Radiation, Laboratory for Applications of Synchrotron Radiation, Kaiserstrasse 12, 76131, Karlsruhe, Germany
[j] AGH University of Science and Technology, Faculty of Physics and Applied Computer Science, Al. Mickiewicza 30, 30-059, Krakow, Poland

ARTICLE INFO

*Keywords:*
Edible mushrooms
HgSe complex
Imaging of the elemental distribution
LA-ICP-MS
μ-XRF
XAS

ABSTRACT

This study provides information on mercury (Hg) localization, speciation and ligand environment in edible mushrooms: *Boletus edulis*, *B. aereus* and *Scutiger pes-caprae* collected at non-polluted and Hg polluted sites, by LA-ICP-MS, SR-μ-XRF and Hg $L_3$-edge XANES and EXAFS. Mushrooms (especially young ones) collected at Hg polluted sites can contain more than 100 μg Hg $g^{-1}$ of dry mass. Imaging of the element distribution shows that Hg accumulates mainly in the spore-forming part (hymenium) of the cap. Removal of hymenium before consumption can eliminate more than 50% of accumulated Hg.

Mercury is mainly coordinated to di-thiols (43–82%), followed by di-selenols (13–35%) and tetra-thiols (12–20%). Mercury bioavailability, as determined by feeding the mushrooms to Spanish slugs (known metal bioindicators owing to accumulation of metals in their digestive gland), ranged from 4% (*S. pes-caprae*) to 30% (*B. aereus*), and decreased with increasing selenium (Se) levels in the mushrooms. Elevated Hg levels in mushrooms fed to the slugs induced toxic effects, but these effects were counteracted with increasing Se concentrations in the mushrooms, pointing to a protective role of Se against Hg toxicity through HgSe complexation. Nevertheless, consumption of the studied mushroom species from Hg polluted sites should be avoided.

## 1. Introduction

The fundamental role of fungi in ecosystems involves organic and inorganic transformations and element cycling, rock and mineral transformations, bio-weathering, fungal–clay interactions, metal-fungal interactions, and mycogenic mineral formation (Falandysz and Borovička, 2013). In addition to these important roles which support maintaining equilibrium in ecosystems, the fruiting bodies of certain fungal species, i.e., mushrooms, are edible, and thus an important nutritional source for forest animals and humans. Wild-growing mushroom consumption has been preferred to cultivated species in many countries, especially in Europe, Asia and America (Choma et al., 2018; Kalač, 2013).

Wild growing mushrooms contain several essential elements and

*Abbreviations:* LA-ICP-MS, Laser Ablation-Inductively Coupled Plasma-Mass Spectrometry; μ-XRF, micro X-ray Fluorescence Spectrometry; XAS, X-ray Absorption Spectroscopy; MeHg, Methyl Mercury; EXAFS, Extended X-ray Absorption Fine Structure; XANES, X-ray Absorption Near Edge Structure; HP, Hepatopancreas; M, Muscle tissues; PTWI, Provisional Tolerable Weekly Intake

* Corresponding author. Katarina Vogel Mikuš University of Ljubljana, Biotechnical faculty, Department of biology, Jamnikarjeva 101, SI-1000, Ljubljana, Slovenia.
*E-mail address:* katarina.vogelmikus@bf.uni-lj.si (K. Vogel-Mikuš).

[1] both authors contributed equally.

https://doi.org/10.1016/j.ecoenv.2019.109623
Received 7 July 2019; Received in revised form 16 August 2019; Accepted 28 August 2019

various organic compounds such as proteins and amino acids, lipids, carbohydrates, vitamins, phenolic compounds, pigments and flavor and taste compounds (Choma et al., 2018; Kalač, 2013). Yet, mushrooms can also accumulate hazardous metals (Hg, Cd, Pb, As) (Alonso et al., 2000; Byrne et al., 1976; Kalač, 2010), and other elements (Se, Ag, Au, Cs, Rb, V, Zn) (Byrne et al., 1976; Kalač, 2010), as well as radionuclides (Falandysz et al., 2015a), especially when grown at polluted sites.

*Boletus edulis* Bull. (king bolete), *Boletus aereus* Bull. (bronze bolete or queen bolete) and *Scutiger (Albatrellus) pes-caprae* (Pers.) Bondartsev & Singer (goat's foot) are edible mushrooms which form mycorrhizal associations with hardwoods and conifers. Mushrooms from the genus *Boletus* spp. can accumulate significant amounts of mercury (Hg, 0.73–6.3 μg $g^{-1}$ dry mass (DM)) (Falandysz, 2008; Kalač, 2013) compared to other mushroom species, even in background environments (Falandysz et al., 2014b; Falandysz and Borovička, 2013). Mercury is considered to be largely in inorganic form (> 80%–99%) (Falandysz et al., 2014b; Miklavčič et al., 2013b), with only a minor portion (up to 5–8%) present as methylmercury (MeHg) (Rieder et al., 2011). Almost no data exist on the bioavailability and toxicity of Hg complexes in mushrooms and risks associated with their consumption. In our previous study on Hg speciation and ligand environment in plants and mycorrhiza, X-ray absorption spectroscopy (XAS) analysis showed that in plants Hg is mainly bound into di-thiolate complexes, while in mycorrhiza tetra-thiolate complexes were detected, resembling Hg binding to fungal metallothioneins (Kodre et al., 2017). Mercury can also bind to amino groups of plant and fungal proteins (Kodre et al., 2017). In mushroom hunting populations, elevated consumption levels (> 100 g mushrooms/week) could lead to exposure to relatively high Hg levels during mushroom hunting season, and as such potential toxicological issues cannot be ignored.

Unlike the majority of edible mushrooms, *Boletus* spp., and especially *S. pes-caprae*, are known selenium (Se) accumulators (Falandysz, 2013, 2008; Kalač, 2013; Liu et al., 2016), with up to 50 and 370 μg Se $g^{-1}$ DM, respectively (Falandysz, 2013; Stijve et al., 1998). The physiological role of Se in these fungi is not known, in particular since in higher fungi, as well as in higher plants, the machinery for the synthesis of selenoproteins was completely lost during evolution. Cysteine-containing homologs of some selenoproteins are utilized instead (Lobanov et al., 2009). However, Se may be taken up inadvertently via sulphate transporters and incorporated into proteins instead of sulphur, leading to synthesis of non-functional Se containing proteins. Despite no apparent physiological role, there are several reports on their antioxidative and protective action in plants (White, 2016). According to research on mammals, Se may also protect against Hg induced stress (Boening, 2000; Byrne et al., 1995; Cuvin-Aralar and Furness, 1991; Spiller, 2018) through conversion of $Hg^{2+}$ ions to insoluble HgSe complexes (Falnoga et al., 2006; Zhang et al., 2014), or through improved antioxidant activity (Zwolak and Zaporowska, 2012). Selenium was shown to inhibit the uptake of MeHg as well as inorganic Hg in rice when applied as soil fertilizer (Zhang et al., 2012). In marine mammals and sea birds, a molecular mechanism that involves formation of an insoluble, equimolar HgSe complex makes Hg biologically unavailable and explains the protective role of Se (Thangavel et al., 1999; Zhang et al., 2014; Zhao et al., 2013, 2004). A HgSe complexation process was also proposed by Shanker et al. (1996), showing a lower Hg uptake in the presence of selenite/selenate in hydroponically treated tomato and radish plants.

Mushrooms are readily consumed by snails and slugs, from the cap and gills or tubes all the way through the entire stipe (Ebenso et al., 2013). Snails and slugs account for an important part of the herbivorous and detrivorous fauna in numerous terrestrial ecosystems and are relevant ecological bioindicators of environmental pollution since they accumulate metals from food in the digestive gland (hepatopancreas) (Berger and Dallinger, 1993; Boshoff et al., 2015; Ebenso et al., 2013). European legislation (European Directive, 2010/63/EU) has strongly limited the use of test animals for scientific purposes (Barré-Sinoussi and Montagutelli, 2015); however, in bioavailability and toxicity studies and testing, living organisms can hardly be replaced by artificial chemical systems. With a persistent need for food security, invertebrates, more specifically slugs, act as an excellent legislation-excluded link between lower (i.e. plants) and higher (i.e. birds, mammals) trophic levels of food chains. Due to their susceptibility to environmental changes they are the environmental bio-indicators of choice to study metal accumulation, bioavailability and toxicity (Morley et al., 2013; Vaufleury and Bispo, 2000).

Development of synchrotron-based spectroscopy techniques such as X-ray Absorption Near Edge Structure (XANES) and Extended X-ray Absorption Fine Structure (EXAFS) has opened new possibilities to study the chemical speciation and ligand environment in biological materials, without the use of extraction procedures that can alter the “in-vivo” ligand state (Kodre et al., 2017; Vogel-Mikuš et al., 2010). The aim of this study was to provide novel information on the localization and chemical speciation of Hg in caps of *B. aereus*, *B. edulis* and *S. pes-caprae* by LA-ICP-MS (Laser Ablation-Inductively Coupled Plasma-Mass Spectrometry), μ-XRF (micro-X-ray Fluorescence Spectrometry) and XANES/EXAFS. The bioavailability of Hg was investigated by feeding mushrooms to Spanish slugs (*Arion vulgaris* L.), following a hypothesis that in mushrooms with higher Se levels, lower Hg bioavailability, bioaccumulation and toxicity in the slug's hepatopancreas will be observed due to formation of insoluble HgSe complexes.

## 2. Materials and methods

### 2.1. Mushroom sampling

Mushrooms of young and/or mature *B. edulis* and *B. aereus* were sampled in September 2014, 2015 and 2016 at non-polluted sites across Slovenia with prevailing Dinaric silver fir-beech and oak forests (Dragomer, 46°01′28.0″N 14°22′19.7″E, Litija, 46°03′50.0″N 14°47′32.7″E, Ilirska Bistrica, 45°34′44.0″N 14°16′18.9″E, Črna na Koroškem, 46°27′50.8″N 14°50′30.6″E), and at a Hg-polluted area near Idrija (46°00′43″N, 14°02′06″E). *S. pes-caprae* was sampled in suburbs of Ljubljana (Dragomer, 46°01′28.0″N 14°22′19.7″E) in acidophilic beech forests.

The fruiting bodies were roughly cleaned in the forest and immediately transferred to the laboratory (University of Ljubljana, Biotechnical faculty, Department of biology) for further treatment. The fruiting bodies were rinsed with Milli-Q water and gently blotted with paper towels. For LA-ICP-MS/μ-XRF analyses, 2 mm thick, flat slices were prepared from the caps, wrapped in Al-foil, frozen in propane cooled by liquid nitrogen, and freeze-dried for three days (Alpha 2–4, Christ) (Vogel-Mikuš et al., 2014). The remaining cap and stipe were also frozen and freeze-dried for bulk Hg and Se analysis.

### 2.2. Bulk elemental analysis

The freeze-dried mushrooms (caps and stipes separately) were pulverized in a mortar with liquid nitrogen. The powder was analysed by ICP-MS for Hg and Se after microwave-assisted acid digestion of 100 mg aliquots in 3 ml $HNO_3$ (CEM MARS-X, USA) (Debeljak et al., 2018). The digests were diluted to 5 ml. One-ml aliquots were stabilized by 750 μL of 38% HCl and 250 μL of 65% $HNO_3$ and diluted with Milli-Q water to 10 ml. Ge, Ga, Y and Sc (5 mg/L, Sigma, Aldrich) were used as internal standards. Standard reference material NIST SRM 1573a (tomato leaves) and Tuna fish BCR627 (Sigma-Aldrich) were used for quality assurance and validation of the analytical procedures.

### 2.3. Laser ablation inductively coupled plasma mass spectrometry and μ-XRF imaging

LA-ICP-MS analysis was performed at the National Institute of Chemistry in Ljubljana (Slovenia), using a 193 nm ArF* excimer laser

ablation system (Analyte G2, Teledyne Photon Machines Inc., Bozeman, MT) coupled to a quadrupole ICP-MS instrument (Agilent 7900×, Agilent Technologies, Santa Clara, CA). Ablation took place in a HelEx 2-volume ablation cell and the mass spectrometer was used in time-resolved analysis mode, measuring one point per mass and acquiring the elements of interest. Parallel line scans were made to construct element maps using the following LA-ICP-MS conditions: fluence, 1.26 J $cm^{-2}$; beam size, 50 µm (round mask); repetition rate, 10 Hz; scanning speed, 100 µm $s^{-1}$; duty cycle time, 0.5 s; measured nuclides, $^{82}Se$, $^{202}Hg$; dwell times (0.04 s and 0.016 s, respectively).

XRF imaging was performed at the XRF beamline of Synchrotron Elettra, Trieste (Karydas et al., 2018). The energy was set at 13.5 keV. X-ray fluorescence was detected by a silicon drift detector (SDD) (Bruker Nano GmbH, XFlash 5030) with a 25 $mm^2$ effective crystal area and a Super Light Element Window (SLEW; Bruker Nano GmbH), placed on the incident beam horizontal plane, perpendicular to the primary beam (Karydas et al., 2018). The samples were scanned with a step size 200 × 100 µm and the counting time was 10 s per step.

The LA-ICP-MS element distribution maps were quantified according to Zidar et al. (2016) and the µ-XRF maps were quantified according to Kump and Vogel-Mikuš (2018).

### 2.4. X-ray absorption spectroscopy

The mushroom and slug samples were prepared for XAS analysis by rapid freezing of the material in liquid nitrogen and subsequent freeze-drying in order to concentrate the samples for their measurement in fluorescence mode. The dried material was ground in a mortar with liquid nitrogen, pressed into self-standing pellets, and stored in vacuum-sealed bags at 4 °C until analysis. In addition, pellets of different Hg compounds were prepared: HgS, HgSe and Hg-phosphate, and most notably, organic Hg complexes with histidine, cysteine, and cellulose as reference standards for N-, S-, and O-ligand environments (Kodre et al., 2017). For preparation of Hg with tetra-thiolate coordination $Hg(S\text{-}R)_4$, typically found in mycorrhiza, a dark-septate endophyte fungus was grown in $HgCl_2$-enriched medium as described in Kodre et al. (2017). In this reference sample (labelled Hg-Fung), 64% of Hg is coordinated as $Hg(S\text{-}R)_4$, 24% as $Hg(N\text{-}R)_2$ and 13% as $Hg(S\text{-}R)_2$.

Hg $L_3$-edge (12,284 eV) XANES and EXAFS spectra of mushroom and slug samples and of standard reference compounds were measured at liquid helium temperature in fluorescence detection mode at the BM30B beamline of the ESRF synchrotron source in Grenoble, France, using a He cryostat and a 30-segment germanium solid state detector to collect the fluorescence signal. The cryo-mode was chosen to improve the signal-to noise ratio and the resolution of interatomic distances (Kodre et al., 2017; Nagy et al., 2011). An arsenic filter was placed in front of the Ge detector to eliminate the elastic scattering peak and to additionally improve the signal-to-noise ratio of the Hg $L_\alpha$ fluorescence line. A Si(220) double crystal monochromator was used with energy resolution of about 1.5 eV at 12 keV. Higher-order harmonics were effectively eliminated by the flat Rh-coated mirror installed downstream of the monochromator. The intensity of the monochromatized beam was monitored with three ionization detectors filled with argon (220 mbar, 754 mbar, and 1600 mbar) and helium to a total pressure of 2 bar. Samples were placed between the first pair of detectors, and the reference tungsten metal foil between the posterior pair to obtain the exact energy calibration (W $L_1$ absorption edge: 12,098 eV). The absolute energy reproducibility of the measured spectra was ± 0.02 eV. The absorption spectra were measured within the interval from −250 eV to 1000 eV relative to the edge. In the XANES region, equidistant energy steps of 0.3 eV were used, while in the EXAFS region equidistant k-steps ($\Delta k \approx 0.03$ $Å^{-1}$) were adopted, with an integration time of 1s/step in transmission mode (reference compounds), and 4s/step in fluorescence detection mode (mushroom and slug samples). The spectra of two to ten identical runs were superimposed to improve the signal-to-noise ratio and to check the stability and reproducibility of the detection system.

Some of the XANES and EXAFS spectra for mushroom and reference samples were recorded at the P64 beamline of PETRA III at DESY (Hamburg, Germany). A Si(111) double crystal monochromator was used with energy resolution of about 1.5 eV at 12 keV. Higher-order harmonics were effectively eliminated by the flat Rh-coated mirror installed downstream from the monochromator. The intensity of the monochromatic X-ray beam was measured by two consecutive 5 cm long ionization chambers, the first one filled with 20% of Kr and 80% $N_2$, and the second one filled with Kr, at 1 bar. The samples were mounted on the sample holder placed after the first ionization detector. For mushroom samples with low Hg concentration (< 50 µg $g^{-1}$ dry weight), the fluorescence detection mode was used, exploiting a large area PIPS detector with 3 µm Ga filter, to measure the intensity of the Hg-$L_\alpha$ fluorescence line. The absorption spectra were measured in the energy region from −150 eV to +1000 eV relative to the Hg $L_3$-edge in continuous scan mode. The scan duration was 300 s. The signal from the detectors was integrated during scanning in the time domain to obtain energy steps of 0.5 eV. Three to five repetitions were superimposed to improve the signal-to-noise ratio. Exact energy calibration of the monochromator was obtained on the Se K-edge by absorption measurements on the selenate reference compound (previously calibrated with the W $L_1$ absorption edge).

Some samples were measured also at the XRF beamline of Synchrotron Elettra, Trieste, in XANES fluorescence mode across the Hg $L_3$-edge, with the set-up as described in Karydas et al. (2018). X-ray fluorescence was measured by a silicon drift detector (SDD) (Bruker Nano GmbH, XFlash 5030) and the X-ray fluorescence signal was normalized according to the signal from the beam monitoring system (Karydas et al., 2018). Energy calibration was performed by measuring the HgS reference compound previously measured at BM30b and calibrated according to the W $L_1$ absorption edge. The counting time per energy step (0.5 eV) was 30 s, while the energy range was from −50 eV to 150 eV around the Hg $L_3$-edge.

The analysis of XANES and EXAFS spectra was performed with the DEMETER (IFEFFIT) program package (Ravel and Newville, 2005), in combination with the FEFF6 program code (Rehr et al., 1992) for *ab initio* calculation of photoelectron scattering paths.

### 2.5. Bioavailability of Hg and Se

Bioavailability was determined by feeding the mushrooms collected at the Idrija and non-polluted sites to Spanish slugs (*Arion vulgaris* L.). Slugs are known metal bioindicators owing to accumulation of metals in their digestive gland, the hepatopancreas (Gimbert et al., 2016). Slugs of comparable size were collected from a non-polluted area near Ljubljana. The slugs in the control group were immediately sacrificed and dissected. Muscle tissue and hepatopancreas were isolated, rapidly frozen in liquid nitrogen, freeze-dried and analysed for background Hg and Se concentrations by ICP-MS after acid digestion as described above. For bioavailability experiments the slugs were placed into plastic containers (φ = 9 cm, volume 0.57 l) containing gypsum (4 cm) and 1% of powdered charcoal (to retain moisture and prevent the growth of microorganisms), and covered by a perforated plastic cover (Fig. S1). The slugs were kept under controlled conditions (22 °C, 16/8 day/night period) and fed for 14 days with pellets pressed from aliquots of 100 mg of freeze-dried powdered mushroom material containing various amounts of Hg and Se. The pellets (φ = 1 cm) were introduced daily in small Petri dishes (φ = 3.5 cm). The pots were moistened with Milli-Q water and cleaned daily. At the end of the experiment the slugs were sacrificed, their muscle tissue and hepatopancreas isolated and analysed for Hg and Se contents by ICP-MS as previously described. The bioaccumulation index (BI) was calculated as follows:

$$\mathrm{BIslug}\,[\%] = \frac{Sslug}{Sfeed} * 100 \qquad (1)$$

where $S_{feed}$ is the Hg content [μg] in consumed feed, the product of Hg concentration in the mushroom [μg $g^{-1}$] and the amount of consumed feed [g]), and $S_{slug}$ is the Hg content [μg] in the slug's hepatopancreas (HP) or muscles tissues (M), the product of Hg concentration [μg $g^{-1}$] in HP or M and dry biomass of HP or M [g]. M/HP Hg and Se concentration ratios were calculated as the ratios between Hg or Se M and HP concentrations.

Malondialdehide (MDA) levels were measured in 80 mg aliquots of fresh HP tissues extracted with 2 mL of 80% ethanol according to Hodges et al. (1999), to determine the level of lipid peroxidation as an indicator of membrane damage due to Hg toxicity.

### 2.6. Statistical analysis

In a one-way ANOVA test the effects of different slug exposures were compared followed by Duncan's post hoc test (Statistica, Statsoft 7.0). Differences at $p < 0.05$ were considered significant. Two-way clustering analysis based on Euclidian distances with a heat chart of "z transformed" parameters obtained from ICP-MS and XANES/EXAFS analysis was performed in the "R" project for statistical computing (i386 3.4.3) (Singh et al., 2014).

## 3. Results and discussion

### 3.1. Accumulation and localization of Hg and Se in mushrooms

*Boletus edulis*, *B. aereus* and *S. pes-caprae* were sampled at different non-polluted and Hg-polluted locations in Slovenia. In non-polluted locations the highest Hg concentration of up to 93 μg $g^{-1}$ DM was found in young fruiting bodies of *S. pes-caprae* (Table 1), far above concentrations found in other mushroom species accumulating Hg in a background environment (Falandysz, 2010; Falandysz et al., 2015b). *S. pes-caprae* is otherwise known as selenium hyperaccumulator (Falandysz, 2010; Stijve et al., 1998), with some evidence that Hg and Se may be co-accumulated in a species-dependent way (Falandysz, 2010). In *Boletus* spp. from non-polluted locations, Hg concentrations of up to 10 μg $g^{-1}$ DM were detected, again in young fruiting bodies (Table 1). The concentrations measured in mushrooms collected at non-polluted sites are comparable to those from Italy, Poland and Spain (Falandysz and Borovička, 2013), while in the Hg-contaminated region of Idrija up to 10 times higher concentrations were found (Table 1), with some specimens exceeding 100 μg Hg $g^{-1}$ of DM.

For humans, the provisional tolerable weekly intake (PTWI) for inorganic mercury is 4 μg $kg^{-1}$ body weight (BW) and for MeHg 1.6 μg $kg^{-1}$ BW (WHO/JECFA, 2007), i.e., 280 and 112 μg, respectively, for a 70-kg person per week. Consumption of a portion of fresh mushroom caps (100 g/week), containing 90% water, and originating from a non-polluted environment, can thus contain 30–110 μg (*Boletus* spp.) and 400–1000 μg Hg (*Scutiger*), the latter highly exceeding the PTWI. A portion of *Boletus* spp. mushrooms from a Hg-contaminated site can contain 440–1150 μg of Hg, exceeding the PTWI four times. Picking and consummation of *Boletus* spp. mushrooms from Hg-polluted sites should therefore be avoided.

Mushroom caps contained typically higher Hg concentrations than stipes (Table 1), as reported previously (Falandysz, 2010). Localization studies using LA-ICP-MS and μ-XRF (Fig. 1) revealed, however, that the spore bearing part (hymenium) is the main Hg accumulation site in the cap already in young fruiting bodies (Fig. S2). Hymenium is the most metabolically active part of the sporocarp, providing nutrients for developing spores during sporulation (Gooday, 1982). Accumulation of essential elements in this part thus enables normal enzyme functioning, while accumulation of non-essential elements like Hg can be considered as inadvertent, utilizing transport pathways of essential elements or transporting to hymenium bound to organic compounds such as sulphur- or selenium-rich proteins. From a consumer's point of view, removing hymenium from the collected mushroom caps can eliminate more than 50% of Hg accumulated in the fruiting body.

Most of around 200 edible mushroom species (belonging to 21 families and 56 genera) contain relatively low Se concentrations (Falandysz and Borovička, 2013). *Boletus* spp. and *Scutiger pes-caprae* are known to accumulate relatively high amounts of Se, which was confirmed also in this study (Table 1). Selenium accumulated mainly in the caps, with higher levels again observed in hymenium of mature sporocarps. The same pattern was found also in young mushrooms of *S. pes-caprae* (Fig. S2b), but less pronounced in young *B. edulis* (Fig. S2a). As such the studied mushroom species could be a good source of dietary Se. A portion of 100 g of fresh mushrooms per week containing 5 μg $g^{-1}$ fresh mass (*Boletus* spp.) could cover 130% of the weekly Se recommended intake of 385 μg (Hartikainen, 2005). However, for *Scutiger*, containing up to ten times more Se, care should be taken not to induce Se toxicity. Similarly as in *Boletus* spp., a large portion of Se could be removed by detaching the hymenium.

### 3.2. XAS analysis of mercury speciation and ligand environment in mushrooms

Hg $L_3$-edge XANES and EXAFS spectra were measured in selected mushroom samples to examine a likely connection between Hg speciation or ligand environment with Hg bioavailability and toxicity. We hypothesized that complexation of Hg with Se may lower the Hg bioavailability and toxicity for mushroom consumers. However, in the literature no direct evidence could be found for the presence of HgSe complexes in higher fungi, despite several works on Hg and Se accumulation in various mushroom species (Falandysz, 2013, 2008; Falandysz et al., 2014a, 2014b; Falandysz and Drewnowska, 2015; Falandysz and Frankowska, 2003).

The relative $L_3$-shell contribution in the absorption spectra was obtained by subtraction of the extrapolated best-fit linear function

**Table 1**
Mercury (Hg) and selenium (Se) concentrations in mushroom caps and stipes collected at non-polluted (NP) sites across Slovenia and a Hg-polluted site in Idrija, measured by ICP-MS (mean ± standard error, n = 2–5).

| | | | Hg (μg $g^{-1}$ DM) | Se (μg $g^{-1}$ DM) |
|---|---|---|---|---|
| *B. edulis* | NP | Cap - mature (n = 5) | 5.79 ± 1.36 | 47.5 ± 3.50 |
| | | Stipe - mature (n = 5) | 2.85 ± 0.64 | 29.4 ± 2.41 |
| | | Cap - young (n = 4) | 10.0 ± 3.49 | 44.7 ± 1.14 |
| | Hg polluted (Idrija) | Cap - mature (n = 2) | 69.0 ± 14.8 | 28.2 ± 10.9 |
| | | Stipe - mature (n = 2) | 14.7 ± 3.40 | 14.4 ± 1.90 |
| | | Cap - young (n = 2) | 103 ± 7.60 | 32.0 ± 3.40 |
| *B. aereus* | NP | Cap - mature (n = 2) | 5.55 ± 0.15 | 45.6 ± 10.5 |
| | | Stipe - mature (n = 2) | 2.59 ± 0.27 | 27.2 ± 5.05 |
| | Hg polluted (Idrija) | Cap - mature (n = 2) | 39.3 ± 5.65 | 9.65 ± 1.85 |
| | | Stipe - mature (n = 2) | 20.1 ± 2.0 | 10.0 ± 0.45 |
| *Scutiger pes-caprae* | NP | Whole - mature (n = 2) | 41.9 ± 2.25 | 246 ± 61.0 |
| | | Whole - young (n = 2) | 92.6 ± 18.4 | 464 ± 12.2 |

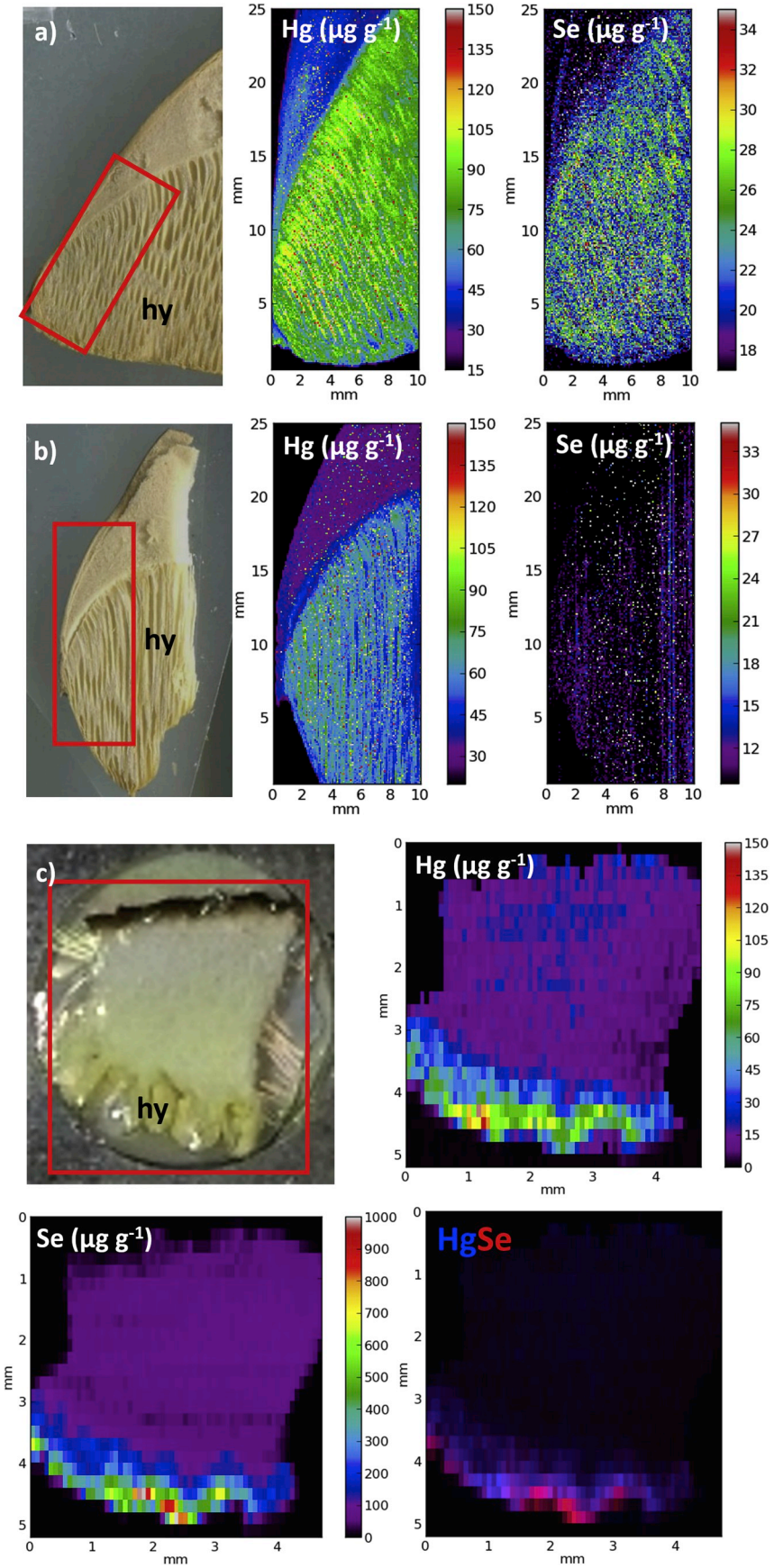


**Fig. 1.** a) Mercury and selenium localization in mature sporocarps of a) *Boletus edulis*, b) *Boletus aereus* and c) *Scutiger pes-caprae.* a, b – LA-ICP-MS, lateral resolution 50 µm × 50 µm, c – µ-XRF, lateral resolution 200 µm × 100 µm. Hy-hymenium. Coloured vertical bars represent concentration (µg $g^{-1}$ DM). Image in the bottom right corner represents colocalization between Hg (blue channel) and Se (red channel). (For interpretation of the references to colour in this figure legend, the reader is referred to the Web version of this article.)

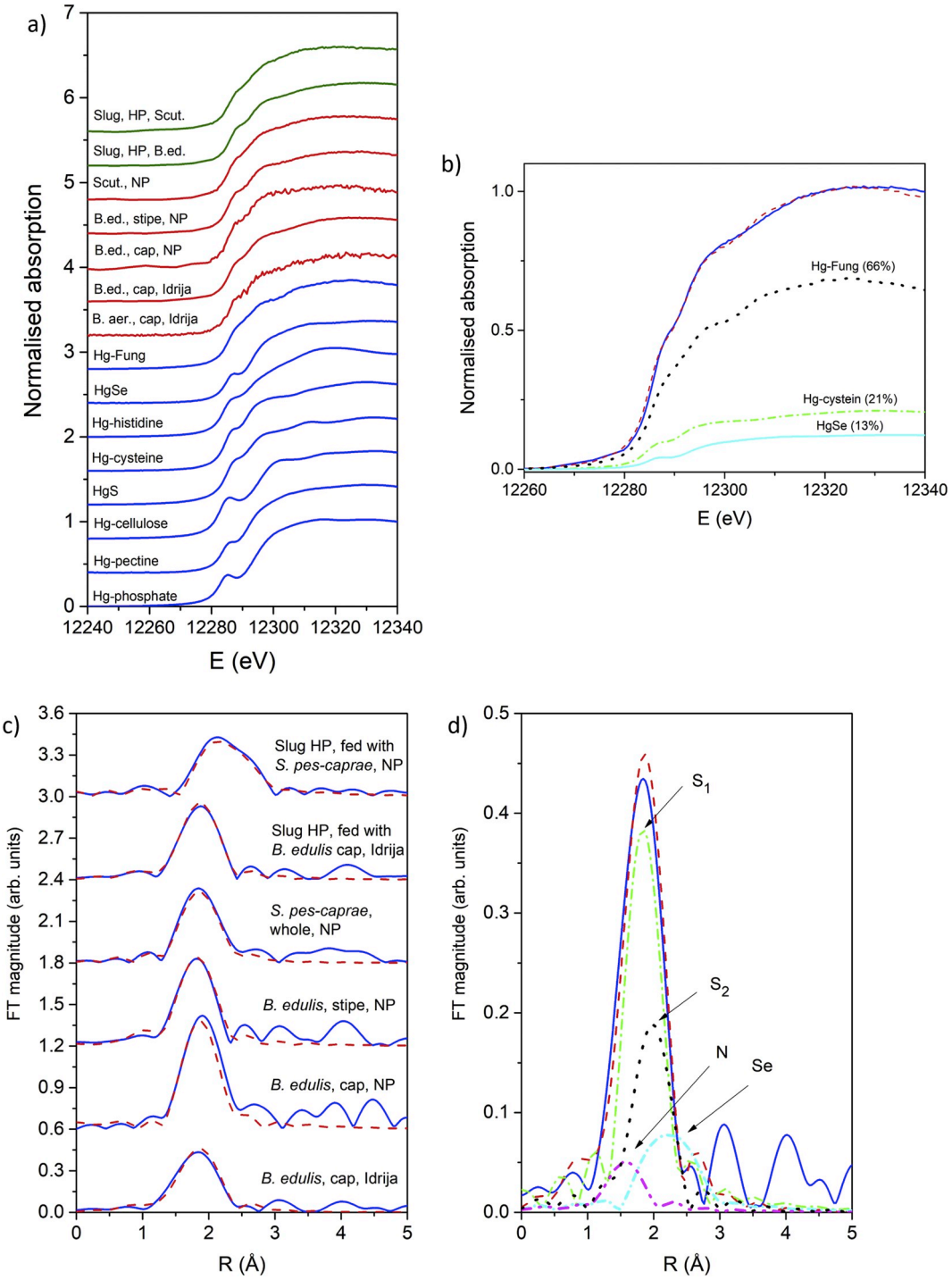


**Fig. 2. a)** Hg $L_3$-edge XANES spectra of Hg reference compounds (blue line), mushrooms (red line) and slug hepatopancreas (green line). The spectra are displaced vertically for clarity. HP- hepatopancreas, NP – non-polluted, B. ed. – *Boletus edulis*, B. ae. – *Boletus aereus*, Scut. – *Scutiger pes-caprae*. **b)** The Hg $L_3$- XANES spectrum measured on *B. edulis* cap (Idrija) sample. Blue line – experiment; red dashed line – best-fit linear combination with XANES profiles: 66% of fungal sample Fung, 21% of Hg-cysteine and 13% of HgSe. **c)** Fourier transform magnitudes of the k weighted Hg $L_3$-edge EXAFS spectra of the mushroom and slug hepatopancreas (HP) samples (blue solid line), together with the best-fit EXAFS model (red dashed line). The spectra are displaced vertically for clarity. **d)** Fourier transform magnitudes of the k weighted Hg $L_3$-edge EXAFS spectrum measured on *B. edulis* cap (Idrija) sample (blue solid line), together with the best-fit EXAFS model (red dashed line), and the contributions of individual neighbour shells: sulphur from di-thiolate Hg complex (green dash–dot line); sulphur from tetra-thiolate Hg complex (black dot line); nitrogen (magenta dash–dot–dot line); selenium (cyan dash-dot line). (For interpretation of the references to colour in this figure legend, the reader is referred to the Web version of this article.)

determined in the pre-edge region (−150 eV to −30 eV), and by conventional normalization, extrapolating the post-edge spline background, determined in the range from 100 eV to 250 eV (to set the Hg $L_3$-edge jump to 1). The spectra are plotted in Fig. 2a, together with a selected set of XANES spectra of reference Hg complexes. The local environment of the Hg atom bound to different organic or inorganic ligands results in distinct $L_3$-edge profiles. Hg in mushrooms is expected to be coordinated with several ligands and therefore XANES spectra are

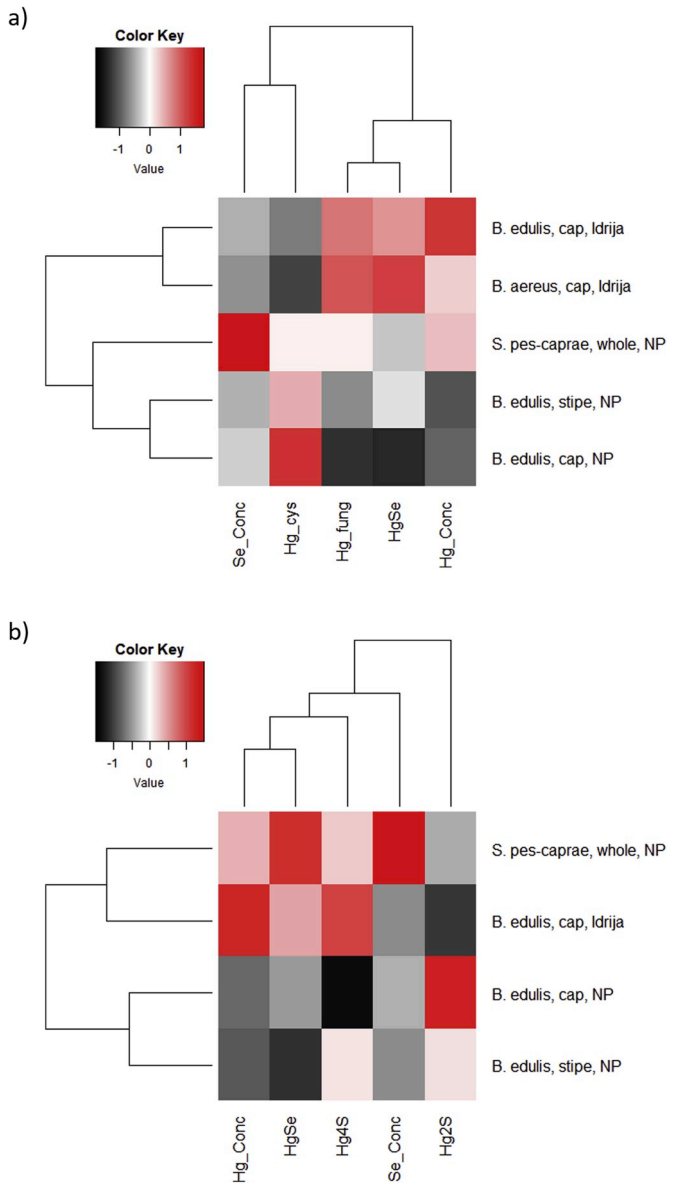


**Fig. 3.** Two-way clustering analysis based on Euclidian distances on "z-transformed" data shows the relationship between Hg ligand environment and Hg and Se mushroom concentrations resulting from **a)** Hg $L_3$-edge XANES and **b)** Hg $L_3$-edge EXAFS analysis. Hg-Conc, Hg concentration in the mushroom (μg $g^{-1}$); Se-Conc, Se concentration in the mushroom (μg $g^{-1}$). Hg2S – $Hg(S\text{-}R)_2$ coordination, Hg4S – $Hg(S\text{-}R)_4$ coordination. For *B. aereus* only XANES was recorded.

expected to exhibit a linear combination of several profiles (Kodre et al., 2017). Three candidates for Hg coordination were identified: Hg-cysteine, Hg-Fung and HgSe, all with known Hg coordination (Kodre et al., 2017). In Hg-cysteine, Hg is mainly coordinated to di-thiolate (84% of $Hg(S\text{-}R)_2$ and 16% $Hg(N\text{-}R)_2$coordination) (Kodre et al., 2017), while in Hg-Fung, the majority of Hg can be found in tetra-thiolate form (fungus cultured in the presence of $HgCl_2$ with 64% of $Hg(S\text{-}R)_4$, 24% of $Hg(N\text{-}R)_2$ and 13% of $Hg(S\text{-}R)_2$ coordination). The relative amounts of individual reference Hg coordinations are obtained by linear combination fits (Fig. 2b). The results are presented in Table S1.

Two-dimensional clustering analysis based on Euclidian distances was performed on "z-transformed" data to link the Hg ligand environment (Hg-cysteine, Hg-Fung and HgSe) to Hg and Se concentrations in mushrooms collected in Hg-polluted and non-polluted environments (Fig. 3a). The results show that increased Hg contents in mushrooms promote Hg coordination to Hg-Fung and HgSe, while in non-polluted environment more Hg is bound in a Hg-cysteine like coordination. As mentioned before, Hg-Fung represents a model coordination similar to tetra-thiolate complexes, as for example in metallothioneins. Sulphur-rich proteins as metallothioneins and phytochelatins are synthesized as a response to elevated metal concentrations and play an important role in metal detoxification. Phytochelatins were recently detected in *B. edulis* and their amount correlated with Cd, Zn, Cu and Hg sporocarp contents (Collin-Hansen et al., 2007).

EXAFS analysis was performed to analyse local structures around Hg atoms in the samples (Fig. 2c). The EXAFS model was built based on our previous study (Kodre et al., 2017), comprising a linear combinations of four Hg model neighbourhood environments: di-thiol ligands $Hg(S\text{-}R)_2$, tetra-thiol ligands $Hg(S\text{-}R)_4$, di-amino ligands $Hg(N\text{-}R)_2$, and di-selenol ligands $Hg(Se\text{-}R)_2$. In view of the short useful k-range of the spectra, cut off at k ~9.5 $Å^{-1}$ by Se K edge, a collective fitting of four spectra at a time was adopted to produce statistically meaningful results: Varying parameters are the relative frequencies (adding up to 1) and the distances R of the neighbours from the central Hg atom, while the widths of the distribution $\sigma^2$ of the neighbour distances are mostly fixed or constrained. A good agreement between the model and the experimental spectra is found in the k range from 2.5 $Å^{-1}$ to 9 $Å^{-1}$ and R range from 1.0 Å to 3.0 Å (Fig. 2c). The list of best fit parameters is given in Table 2. The contributions of the individual neighbour shells: sulphur from di-tholate Hg complex, sulphur from tetra-tholate Hg complex, nitrogen and selenium are illustrated in Fig. 2d for the case of *B. edulis* cap (Idrija) sample.

The EXAFS results are in line with XANES analysis, pointing to an increase in Hg tetra-thiolate and HgSe complexation in mushrooms with higher Hg contents (Fig. 3b) as a response to Hg toxicity in Hg-polluted environments. In non-polluted environments, Hg di-thiolate complexes are more abundant. *Boletus* spp. mushrooms contain up to 1% of sulphur, while in other fungi and plants the sulphur concentration usually ranges from 0.1 to 0.5% (Kavčič et al., 2017). Sulphur speciation studies by high resolution particle induced X-ray emission spectrometry showed a relatively large proportion of thiols, presenting inadvertent binding sites for metal ions as $Hg^{2+}$ (Kavčič et al., 2017). In addition, the presence of HgSe complexes was more frequently observed in the Se hyperaccumulator *S. pes-caprae* (Table 2), suggesting lower Hg bioavailability and toxicity related to this mushroom.

### 3.3. Mercury bioavailability and toxicity

Bioavailability and toxicity of Hg in mushrooms collected in Idrija and in non-polluted environments was evaluated in feeding experiments involving Spanish slugs as a model invertebrate species. A linear correlation was observed between the mean Hg concentration in feed (freeze-dried and pelletized parts of mushrooms, see Table 3), and the mean Hg concentration in hepatopancreas (HP) (Fig. S3a), as already observed in other studies (Boshoff et al., 2015; Gimbert et al., 2016). The relation between Hg in feed and muscle tissue (M) was exponential, with a deviation of the Hg concentration in muscle tissue of slugs fed with *B. aereus* cap (3.19 μg $g^{-1}$ DM) (Fig. S3a, Table 3). High Hg bioavailability from *B. aereus* was also confirmed by the highest bioaccumulation index (BI), calculated from the respective Hg contents in feed and HP or M, and the highest M/HP concentration ratio (Table 3). For *B. aereus*, Hg–BI–HP was 30.2% for HP and 5.2% for M, while for *B. edulis* the ranges were 12.8–16.7% for HP and 0.79–1.85% for M. The lowest values, however, were found for *S. pes-caprae*, correlating with high Se levels and HgSe complexation as confirmed by EXAFS (Table 2). Due to the very strong bonds within HgSe complexes, Hg becomes less bioavailable and less toxic for the consumers. Additionally, high Se levels in food may promote complexation, also within the consumer's digestion system (the slug's hepatopancreas in this case). The transport of Hg from the hepatopancreas to muscle tissues is governed by the mobility of Hg species in the slug organism. The

**Table 2**
Best-fit model parameters of Hg-$L_3$ edge EXAFS spectra of the four mushroom and two slug hepatopancreas (HP) samples. The model comprises four Hg ligands yielding the relative frequencies and bond radii (R); the widths of the distribution ($\sigma^2$) of the bond radii are mostly fixed or constrained. The effective zero energy of the photoelectron $E_0$ is given, together with the quality-of-fit (r-factor). (*) - restricted to a common value, (**) - fixed values. $S_0^2$ is set to 1.0. The uncertainty of the last digit is given in parentheses. NP – non-polluted sites, Idrija – Hg polluted site.

| | *B. edulis* cap Idrija | *B. edulis* cap NP | *B. edulis* stalk NP | *S. pes-caprae* whole NP | Slug HP, fed with *B. edulis* cap, Idrija | Slug HP, fed with *S. pes-caprae*, whole, *NP* |
|---|---|---|---|---|---|---|
| **Di-thiolate Hg complex: $Hg(S\text{-}R)_2$** | | | | | | |
| rel. freq. ($S_1$) | 0.43[7] | 0.82[6] | 0.63[7] | 0.54[6] | 0.60[7] | 0.12[6] |
| R ($S_1$) [Å] | 2.323[8] | 2.323* | 2.323* | 2.323* | 2.323* | 2.323* |
| $\sigma^2$ ($S_1$) [$10^{-4}$Å$^2$] | 13* | 13* | 13* | 13* | 27 | 27** |
| **Tetra-thiolate Hg complex: $Hg(S\text{-}R)_4$** | | | | | | |
| rel. freq. ($S_2$) | 0.19[8] | 0.0 | 0.12[9] | 0.13[8] | 0.20[9] | 0.0 |
| R ($S_2$) [Å] | 2.478[15] | – | 2.478* | 2.478* | 2.478* | – |
| $\sigma^2$ ($S_2$) [$10^{-4}$Å$^2$] | 85** | – | 85** | 85** | 27* | – |
| **Di-amino Hg complex with $Hg(N\text{-}R)_2$ or Hg complex with two N in heterocyclic amines** | | | | | | |
| rel. freq. (N) | 0.13[10] | 0.0 | 0.13[10] | 0.0 | 0.0 | 0.0 |
| R (N) [Å] | 2.035** | – | 2.035** | – | – | – |
| $\sigma^2$ (N) [$10^{-4}$Å$^2$] | 30** | – | 30** | – | – | – |
| **Di-selenol Hg complex: $Hg(Se\text{-}R)_2$** | | | | | | |
| rel. freq. (Se) | 0.28[17] | 0.19[11] | 0.13[9] | 0.35[18] | 0.22[15] | 0.89[11] |
| R (Se) [Å] | 2.615[15] | 2.615* | 2.615* | 2.615* | 2.615* | 2.615* |
| $\sigma^2$ (Se) [$10^{-4}$Å$^2$] | 84** | 84** | 84** | 84** | 84** | 51 |
| E0 [eV] | 4.0* | 4.0* | 4.0* | 4.0* | 5.5 | 5.5** |
| r-factor | 0.040 | 0.087 | 0.036 | 0.017 | 0.022 | 0.060 |

most mobile Hg species in biological systems is MeHg (Rodrigues et al., 2011), so the higher translocation yield from HP to M in slugs fed with *B. aereus* may be attributed either to weaker Hg complexation in HP or to a higher concentration of the highly mobile MeHg. Several studies show that Hg accumulates in muscle tissues of invertebrates as well as vertebrates, including fish and marine mammals, mainly as MeHg (< 95%) (Miklavčič et al., 2013b; Rua-Ibarz et al., 2016; Sadhu et al., 2015; Wagemann et al., 1998). The amount of MeHg found in mushrooms in the vicinity of the Idrija Hg mine can range up to 12% (Miklavčič et al., 2013a). In a study performed in Switzerland, mushroom MeHg contents ranged from 5 to 8%, but *B. edulis*, *B. aereus* and *S. pes-caprae* were not included in the study (Rieder et al., 2011). XAS analysis with a detection limit of ~5% for MeHg was not able to confirm its presence. However, as evident from XANES/EXAFS, there was a difference in Hg complexation in HP of slugs fed by *B. edulis* or *S. pes-caprae*. In slugs fed by *B. edulis*, the majority of Hg was in Hg-di-thiolate form, while in those fed by *S. pes-caprae* almost 90% of Hg was present as HgSe. Elevated mushroom Se levels apparently help to immobilize Hg in the slug's digestive gland.

Slugs fed with mushrooms collected in Idrija exhibited lower muscle tissue biomass at the end of the experiment compared to those fed with mushrooms from non-polluted environments, indicating a cumulative Hg-induced toxicity (Table 3). A reduced growth rate and impaired reproduction were also reported in the Hg-exposed snail *Cantareus aspersus* (Gimbert et al., 2016). Additionally, in our experiment the level of lipid peroxidation was measured in the slug's digestive gland through production of malondialdehyde. Results showed significantly increased levels in slugs fed with mushrooms collected in Idrija (Fig. 4a), while

**Table 3**
Slug dry mass (DM) (hepatopancreas - HP, muscle tissues - M), Hg and Se concentrations (μg $g^{-1}$ DM) and contents (μg) in feed: freeze-dried mushroom cap, stipe or whole, collected in Hg polluted (Idrija) and non-polluted (NP) environments, and slug HP and M contents (μg $organ^{1}$) after 14 days of feeding (mean ± standard error, n = 4–6). HP and M contents are the products of respective DM and Hg or Se concentrations (n = 4–6 per exposure). The letters next to the values represent statistically significant differences (Duncan's test, $p < 0.05$).

| | | Control | *B. aereus* cap, Idrija | *B. edulis* cap, Idrija | *B. edulis* cap, NP | *B. edulis* stipe, NP | *S. pes-caprae* whole, NP |
|---|---|---|---|---|---|---|---|
| Slug DM | HP (g) | 0.068 ± 0.007 c | 0.242 ± 0.026 a | 0.110 ± 0.021 bc | 0.139 ± 0.010 b | 0.140 ± 0.050 b | 0.102 ± 0.017 bc |
| | M (g) | 0.895 ± 0.076 b | 0.560 ± 0.078 c | 0.587 ± 0.088 c | 1.367 ± 0.044 a | 1.140 ± 0.092 a | 0.781 ± 0.121 bc |
| MDA (mmol $g^{-1}$) | HP | 4.25 ± 0.468 d | 9.49 ± 0.445 a | 8.93 ± 0.510 ab | 7.84 ± 0.551 b | 6.82 ± 0.441 c | 6.41 ± 0.410 c |
| Hg | Feed (μg $g^{-1}$ DM) | < 0.05 | 56.0 ± 2.80 c | 98.9 ± 4.95 d | 7.85 ± 0.393 a | 3.72 ± 0.186 a | 30.0 ± 1.5 b |
| | Feed (μg) | < 0.05 | 33.6 ± 3.96 c | 60.1 ± 4.92 a | 18.9 ± 0.373 d | 8.62 ± 0.478 e | 44.1 ± 0.990 b |
| | HP (μg $g^{-1}$ DM) | < 0.05 | 42.2 ± 4.64 b | 94.8 ± 9.13 a | 18.0 ± 2.51 c | 18.4 ± 6.12 c | 18.0 ± 2.51 c |
| | HP (μg $organ^{1}$) | < 0.05 | 10.3 ± 1.84 a | 9.99 ± 1.02 a | 2.42 ± 0.223 b | 1.59 ± 0.449 c | 1.71 ± 0.217 c |
| | M (μg $g^{-1}$ DM) | < 0.05 | 3.19 ± 0.33 a | 1.90 ± 0.217 b | 0.112 ± 0.042 c | 0.129 ± 0.087 c | 0.235 ± 0.102 c |
| | M (μg $organ^{1}$) | < 0.05 | 1.79 ± 0.327 a | 1.11 ± 0.191 a | 0.150 ± 0.056 c | 0.135 ± 0.091 c | 0.197 ± 0.092 b |
| | M/HP conc. ratio | n.d. | 0.075 | 0.020 | 0.006 | 0.007 | 0.013 |
| | BI–HP (%) | n.d. | 30.2% a | 16.7% b | 12.8% b | 18.3% b | 3.89% c |
| | BI–M (%) | n.d. | 5.21% a | 1.85% b | 0.79% b | 1.62% b | 0.445% c |
| Se | Feed (μg $g^{-1}$ DM) | < 0.05 | 13.0 ± 0.650 a | 13.9 ± 0.696 a | 30.0 ± 1.50 b | 14.0 ± 0.71 a | 126 ± 6.30 c |
| | Feed (μg) | < 0.05 | 7.80 ± 0.441 | 8.46 ± 0.346 | 72.0 ± 0.636 | 32.6 ± 0.807 | 185 ± 1.86 |
| | HP (μg $g^{-1}$ DM) | 0.230 ± 0.048 a | 4.64 ± 0.448 c | 5.52 ± 0.231 c | 28.1 ± 2.70 b | 29.2 ± 5.36 b | 87.1 ± 6.42 a |
| | HP (μg $organ^{1}$) | 0.02 ± 0.01 c | 1.15 ± 0.220 c | 0.597 ± 0.089 c | 3.79 ± 0.155 b | 3.60 ± 0.601 b | 8.47 ± 0.930 a |
| | M (μg $g^{-1}$ DM) | 0.121 ± 0.010 d | 1.45 ± 0.140 c | 1.44 ± 0.110 c | 8.48 ± 1.19 b | 10.6 ± 0.650 b | 13.0 ± 0.841 a |
| | M (μg $organ^{1}$) | 0.11 ± 0.02 b | 0.844 ± 0.194 b | 0.852 ± 0.169 b | 11.4 ± 1.39 a | 11.9 ± 0.893 a | 9.77 ± 1.11 a |
| | M/HP conc. ratio | 0.525 | 0.313 | 0.261 | 0.302 | 0.362 | 0.149 |
| | BI–HP (%) | n.d. | 14.4% a | 7.2% bc | 5.3% c | 11.2% ab | 4.6% c |
| | BI–M (%) | n.d. | 10.5% bc | 10.0% bc | 15.9% b | 36.9% a | 5.3% c |

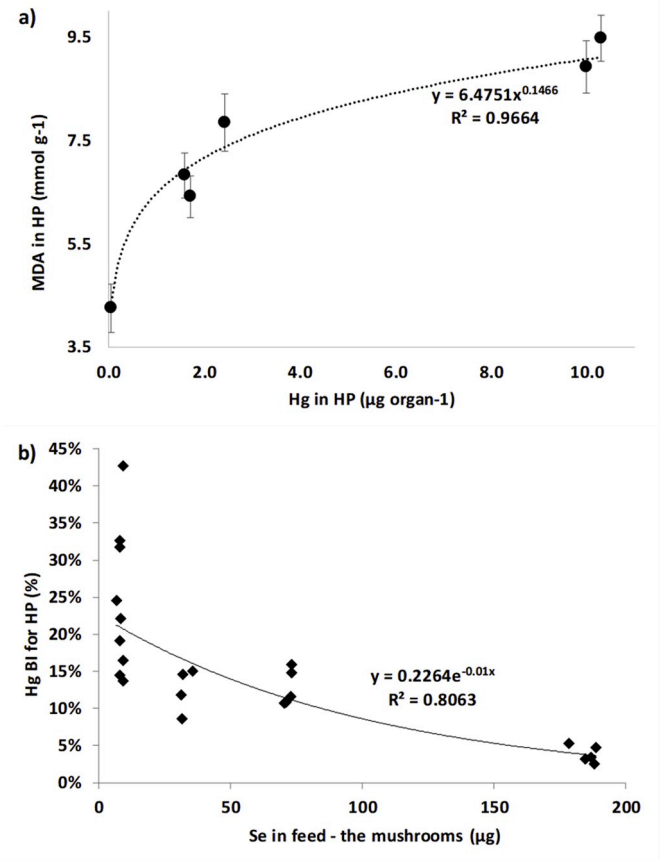


**Fig. 4. a)** Malondialdehyde (MDA) levels in slug hepatopancreas (HP) at different Hg content in HP (µg organ$^{-1}$) (mean ± se, n = 4–6). **b)** The relationship between Hg bioaccumulation index (BI) in hepatopancreas (HP) and the Se content in mushrooms fed to the slugs (presented individual data).

the slugs fed with mushrooms from non-polluted sites were less affected, despite high Hg levels found in *S. pes-caprae*, pointing to a lower Hg toxicity from this Se-hyperaccumulating mushroom.

### 3.4. Effects of selenium on mercury uptake and toxicity

As expected, the highest Se concentrations were found in *S. pes-caprae*, followed by *Boletus* spp. from non-polluted sites and *Boletus* spp. from Idrija (Table 1). Despite being co-localized (Fig. 1), there was no correlation between Se and Hg concentrations in the analysed mushrooms. All collected species are known Se-accumulators, but relatively lower Se levels were found in *Boletus* spp. mushrooms collected in Idrija than in those from non-polluted sites, probably due to differences in soil Se levels (Falandysz, 2013; Hartikainen, 2005; Slekovec and Goessler, 2005; White and Broadley, 2009). Certain areas are low in Se or even Se deficient, resulting in subsequently lower Se contents in the organisms. On the other hand high Hg levels in soil may inhibit Se uptake due to HgSe complexation (Xu et al., 2019), but further studies are needed to better understand the effects of Hg on Se uptake.

Selenium accumulated mainly in the slugs' digestive glands, proportional to the Se concentration in the mushrooms fed to the slugs (Fig. S3b), but relatively more Se than Hg was translocated to the muscle tissues (Table 3), pointing to a higher Se mobility compared to Hg in the slug organism, in line with Se being an essential element for animals (Zwolak and Zaporowska, 2012). The highest Se concentrations were found in HP and M of slugs fed with *S. pes-caprae* (Table 3). Se–BI–HP ranged from 4.6 to 14.4% and Se–BI–M from 5.3 to 36.9%. The lowest Se–BI–M was calculated for slugs fed with *S. pes-caprae*, pointing to a relatively low Se bioavailability in *S. pes-caprae* compared to *Boletus* spp., as reported already by Slejkovec et al. (2000). The relationship between Hg–BI–HP and Se contents (Fig. 4b) clearly indicates that Se lowers the Hg bioavailability and toxicity in the mushroom-slug food chain, confirming Se and Hg antagonism which is of great importance for mushroom consumers. However, based on MDA tests of slugs fed by mushrooms collected at Hg-contaminated sites and calculated PTWI of Hg, consumption of these mushrooms should be avoided.

## 4. Conclusions

- *B. aereus* and *B. edulis* accumulate significant amounts of Hg, especially at Hg-contaminated sites. *S. pes-caprae* accumulates significant amounts of Hg also at non-polluted sites.
- Hg accumulates mainly in the mushroom's caps, more specifically in the spore forming part, the hymenium. By removing the hymenium from the mushroom caps before consumption, more than 50% of Hg can be eliminated.
- Hg in examined mushrooms from non-polluted environments is mainly bound to di-thiolate and di-selenol ligands, while at Hg polluted sites the proportion of di-selenol and tetra-thiol ligands increases. The used XANES/EXAFS methodology is not sensitive enough to detect MeHg in the studied samples.
- Experiments with the Spanish slug show that Hg is present in mushrooms in bioavailable form as it accumulates in the slug's hepatopancreas (BI = 3.9–30.2%), and also in the muscle tissues (BI = 0.45–5.2%), in the latter probably as MeHg.
- Complexation of Hg to Se was confirmed to decrease the Hg bioavailability and toxicity for the consumers, yet suggesting that consumption of the studied mushroom species should be avoided when collected at Hg-contaminated sites.

## Acknowledgement

The study was financed by the Slovenian Research Agency programs (P1-0212, P1-0112, P1-0034 and P3-0395), projects (J7-9418, J7-9398, J1-8156 and N1-0060) and "Young Researcher" grant (A. Kavčič), and by the International Atomic Energy Agency framework of coordinated research projects 1917 "Experiments with Synchrotron Radiation for Modern Environmental and Industrial Applications" (CSI P. Kump, K. Vogel-Mikuš), and also partly supported by the project CALIPSOplus under Grant Agreement 730872 from the EU Framework Program for Research and Innovation HORIZON 2020. The European Synchrotron Radiation Facility (ESRF), Grenoble, France, is acknowledged for provision of synchrotron radiation facilities at beamline BM30B (project EV-210), Synchrotron Elettra Trieste for provision of synchrotron radiation facilities at beamline XRF, (projects 20145060, 20155028, 20165180), and DESY, Hamburg, Germany, a member of the Helmholtz Association, project I-20160764 EC, for provision of synchrotron radiation facilities at beamline P64 of PETRA III. The authors are grateful to ESRF staff Olivier Proux for assistance in using beamline BM30B, and Wolfgang Caliebe and Vadim Murzin from P64 beamline of DESY for expert advice on P64 beamline operation.

## Appendix A. Supplementary data

Supplementary data to this article can be found online at https://doi.org/10.1016/j.ecoenv.2019.109623.

## 5 References

Alonso, J., Salgado, M.J., García, M.a., Melgar, M.J., 2000. Accumulation of mercury in edible macrofungi: influence of some factors. Arch. Environ. Contam. Toxicol. 38, 158–162. https://doi.org/10.1007/s002449910020.

Barré-Sinoussi, F., Montagutelli, X., 2015. Animal models are essential to biological research: issues and perspectives. Futur. Sci. OA 1 fso.15.63. https://doi.org/10.4155/fso.15.63.

Berger, B., Dallinger, R., 1993. Terrestrial snails as quantitative indicators of environmental metal pollution. Environ. Monit. Assess. 25, 65–84. https://doi.org/10.1007/BF00549793.
Boening, D.W., 2000. Ecological effects, transport, and fate of mercury: a general review. Chemosphere 40, 1335–1351. https://doi.org/10.1016/S0045-6535(99)00283-0.
Boshoff, M., Jordaens, K., Baguet, S., Bervoets, L., 2015. Trace metal transfer in a soil–-plant–snail microcosm field experiment and biomarker responses in snails. Ecol. Indicat. 48, 636–648. https://doi.org/10.1016/j.ecolind.2014.08.037.
Byrne, A., Škreblin, M., Falnoga, I., Al-Sabti, K., Horvat, M., 1995. Mercury and selenium perspectives from Idrija. Acta Chim. Slov. 42, 175–198.
Byrne, A.R., Ravnik, V., Kosta, L., 1976. Trace element concentrations in higher fungi. Sci. Total Environ. 6, 65–78. https://doi.org/10.1016/0048-9697(76)90007-3.
Choma, A., Nowak, K., Komaniecka, I., Waśko, A., Pleszczyńska, M., Siwulski, M., Wiater, A., 2018. Chemical characterization of alkali-soluble polysaccharides isolated from a Boletus edulis (Bull.) fruiting body and their potential for heavy metal biosorption. Food Chem. 266, 329–334. https://doi.org/10.1016/J.FOODCHEM.2018.06.023.
Collin-Hansen, C., Pedersen, S.A., Andersen, R.A., Steinnes, E., 2007. First report of phytochelatins in a mushroom: induction of phytochelatins by metal exposure in *Boletus edulis*. Mycologia 99, 161–174. https://doi.org/10.1080/15572536.2007.11832576.
Cuvin-Aralar, M.L., Furness, R.W., 1991. Mercury and selenium interaction: a review. Ecotoxicol. Environ. Saf. 21, 348–364.
Debeljak, M., van Elteren, J.T., Špruk, A., Izmer, A., Vanhaecke, F., Vogel-Mikuš, K., 2018. The role of arbuscular mycorrhiza in mercury and mineral nutrient uptake in maize. Chemosphere 212, 1076–1084. https://doi.org/10.1016/j.chemosphere.2018.08.147.
Ebenso, I.E., Solomon, I.P., Akoje, C.C., Akpan, I.P., Eko, P.M., Akpan, E.A., Omole, A.J., 2013. Bioaccumulation of iron, zinc, cadmium and chromium by juvenile snail Limicolaria aurora J., fed edible mushroom Pleurotus spp from Niger Delta, Nigeria. Bull. Environ. Contam. Toxicol. 90, 314–317. https://doi.org/10.1007/s00128-012-0920-4.
Falandysz, J., 2013. Review: on published data and methods for selenium in mushrooms. Food Chem. 138, 242–250. https://doi.org/10.1016/j.foodchem.2012.10.046.
Falandysz, J., 2010. Mercury in certain mushroom species in Poland. In: Progress in Mycology. Springer Netherlands, Dordrecht, pp. 349–383. https://doi.org/10.1007/978-90-481-3713-8_13.
Falandysz, J., 2008. Selenium in edible mushrooms. J. Environ. Sci. Health C Environ. Carcinog. Ecotoxicol. Rev. 26, 256–299. https://doi.org/10.1080/10590500802350086.
Falandysz, J., Borovička, J., 2013. Macro and trace mineral constituents and radionuclides in mushrooms: health benefits and risks. Appl. Microbiol. Biotechnol. 97, 477–501. https://doi.org/10.1007/s00253-012-4552-8.
Falandysz, J., Drewnowska, M., 2015. Distribution of mercury in Amanita fulva (Schaeff.) Secr. mushrooms: accumulation, loss in cooking and dietary intake. Ecotoxicol. Environ. Saf. 115, 49–54. https://doi.org/10.1016/j.ecoenv.2015.02.004.
Falandysz, J., Dryzałowska, A., Saba, M., Wang, J., Zhang, D., 2014a. Mercury in the fairy-ring of Gymnopus erythropus (pers.) and Marasmius dryophilus (Bull.) P. Karst. Mushrooms from the Gongga mountain, Eastern Tibetan plateau. Ecotoxicol. Environ. Saf. 104, 18–22. https://doi.org/10.1016/j.ecoenv.2014.02.012.
Falandysz, J., Frankowska, A., 2003. Accumulation factors of mercury by king Bolete Boletus edulis. J. Phys. IV 107, 439–442. https://doi.org/10.1051/jp4:20030335.
Falandysz, J., Krasińska, G., Pankavec, S., Nnorom, I.C., 2014b. Mercury in certain boletus mushrooms from Poland and Belarus. J. Environ. Sci. Health. B. 49, 690–695. https://doi.org/10.1080/03601234.2014.922853.
Falandysz, J., Zalewska, T., Krasińska, G., Apanel, A., Wang, Y., Pankavec, S., 2015a. Evaluation of the radioactive contamination in fungi genus Boletus in the region of Europe and Yunnan Province in China. Appl. Microbiol. Biotechnol. 99, 8217–8224. https://doi.org/10.1007/s00253-015-6668-0.
Falandysz, J., Zhang, J., Wang, Y.-Z., Saba, M., Krasińska, G., Wiejak, A., Li, T., 2015b. Evaluation of mercury contamination in fungi Boletus species from latosols, lateritic red Earths, and red and yellow Earths in the circum-Pacific Mercuriferous belt of Southwestern China. PLoS One 10, e0143608. https://doi.org/10.1371/journal.pone.0143608.
Falnoga, I., Tušek-Žnidarič, M., Stegnar, P., 2006. The influence of long-term mercury exposure on selenium availability in tissues: an evaluation of data. BioMetals 283–294. https://doi.org/10.1007/s10534-005-8642-2.
Gimbert, F., Perrier, F., Caire, A.L., de Vaufleury, A., 2016. Mercury toxicity to terrestrial snails in a partial life cycle experiment. Environ. Sci. Pollut. Res. 23, 3165–3175. https://doi.org/10.1007/s11356-015-5632-y.
Gooday, G.W., 1982. Metabolic Control of Fruitbody Morphogenesis in Coprinus Cinereus. Springer, New York, NY, pp. 157–173. https://doi.org/10.1007/978-1-4612-5677-9_8.
Hartikainen, H., 2005. Biogeochemistry of selenium and its impact on food chain quality and human health. J. Trace Elem. Med. Biol. 309–318. https://doi.org/10.1016/j.jtemb.2005.02.009.
Hodges, D.M., DeLong, J.M., Forney, C.F., Prange, R.K., DeLong, J.M., Hodges, D.M., Forney, C.F., Prange, R.K., 1999. Improving the thiobarbituric acid-reactive-substances assay for estimating lipid peroxidation in plant tissues containing anthocyanin and other interfering compounds. Planta 207, 604–611. https://doi.org/10.1007/s004250050524.
Kalač, P., 2013. A review of chemical composition and nutritional value of wild-growing and cultivated mushrooms. J. Sci. Food Agric. 93, 209–218. https://doi.org/10.1002/jsfa.5960.
Kalač, P., 2010. Trace element contents in European species of wild growing edible mushrooms: a review for the period 2000-2009. Food Chem. 122, 2–15. https://doi.org/10.1016/j.foodchem.2010.02.045.
Karydas, A.G., Czyzycki, M., Leani, J.J., Migliori, A., Osan, J., Bogovac, M., Wrobel, P., Vakula, N., Padilla-Alvarez, R., Menk, R.H., Gol, M.G., Antonelli, M., Tiwari, M.K., Caliri, C., Vogel-Mikuš, K., Darby, I., Kaiser, R.B., 2018. An IAEA multi-technique X-ray spectrometry endstation at Elettra Sincrotrone Trieste: benchmarking results and interdisciplinary applications. J. Synchrotron Radiat. 189–203. https://doi.org/10.1107/S1600577517016332.
Kavčič, M., Petric, M., Vogel-Mikuš, K., 2017. Chemical speciation using high energy resolution PIXE spectroscopy in the tender X-ray range. https://doi.org/10.1016/j.nimb.2017.06.009.
Kodre, A., Arčon, I., Debeljak, M., Potisek, M., Likar, M., Vogel-Mikuš, K., 2017. Arbuscular mycorrhizal fungi alter Hg root uptake and ligand environment as studied by X-ray absorption fine structure. Environ. Exp. Bot. 133, 12–23. https://doi.org/10.1016/j.envexpbot.2016.09.006.
Kump, P., Vogel-Mikuš, K., 2018. Quantification of 2D elemental distribution maps of intermediate-thick biological sections by low energy synchrotron μ-X-ray fluorescence spectrometry. J. Instrum. 13. https://doi.org/10.1088/1748-0221/13/05/C05014.
Liu, Y., Chen, Di, You, Y., Zeng, S., Li, Y., Tang, Q., Han, G., Liu, A., Feng, C., Li, C., Su, Y., Su, Z., Chen, Daiwen, 2016. Nutritional composition of boletus mushrooms from Southwest China and their antihyperglycemic and antioxidant activities. Food Chem. 211, 83–91. https://doi.org/10.1016/j.foodchem.2016.05.032.
Lobanov, A.V., Hatfield, D.L., Gladyshev, V.N., 2009. Eukaryotic selenoproteins and selenoproteomes. Biochim. Biophys. Acta 1790, 1424. https://doi.org/10.1016/J.BBAGEN.2009.05.014.
Miklavčič, A., Mazej, D., Jaćimović, R., Dizdarevič, T., Horvat, M., 2013a. Mercury in food items from the Idrija mercury mine area. Environ. Res. 125, 61–68. https://doi.org/10.1016/j.envres.2013.02.008.
Miklavčič, A., Mazej, D., Jaćimović, R., Dizdarevič, T., Horvat, M., 2013b. Mercury in food items from the Idrija mercury mine area. Environ. Res. 125, 61–68. https://doi.org/10.1016/j.envres.2013.02.008.
Morley, E.L., Jones, G., Radford, A.N., 2013. The importance of invertebrates when considering the impacts of anthropogenic noise. Proc. R. Soc. Lond. Biol. Sci. 281, 2013–2683.
Nagy, K.L., Manceau, A., Gasper, J.D., Ryan, J.N., Aiken, G.R., 2011. Metallothionein-like multinuclear clusters of mercury(II) and sulfur in peat. Environ. Sci. Technol. 45, 7298–7306. https://doi.org/10.1021/es201025v.
Ravel, B., Newville, M., 2005. ATHENA, ARTEMIS, HEPHAESTUS: data analysis for X-ray absorption spectroscopy using IFEFFIT. J. Synchrotron Radiat. 12, 537–541. https://doi.org/10.1107/S0909049505012719.
Rehr, J.J., Albers, R.C., Zabinsky, S.I., 1992. High-order multiple-scattering calculations of x-ray-absorption fine structure. Phys. Rev. Lett. 69, 3397–3400. https://doi.org/10.1103/PhysRevLett.69.3397.
Rieder, S.R., Brunner, I., Horvat, M., Jacobs, A., Frey, B., 2011. Accumulation of mercury and methylmercury by mushrooms and earthworms from forest soils. Environ. Pollut. 159, 2861–2869. https://doi.org/10.1016/j.envpol.2011.04.040.
Rodrigues, S.M., Henriques, B., Reis, a.T., Duarte, a.C., Pereira, E., Römkens, P.F.a.M., 2011. Hg transfer from contaminated soils to plants and animals. Environ. Chem. Lett. 10, 61–67. https://doi.org/10.1007/s10311-011-0329-z.
Rua-Ibarz, A., Bolea-Fernandez, E., Maage, A., Frantzen, S., Valdersnes, S., Vanhaecke, F., 2016. Assessment of Hg pollution released from a WWII submarine wreck (U-864) by Hg isotopic analysis of sediments and *Cancer pagurus* tissues. Environ. Sci. Technol. 50, 10361–10369. https://doi.org/10.1021/acs.est.6b02128.
Sadhu, A.K., Kim, J.P., Furrell, H., Bostock, B., 2015. Methyl mercury concentrations in edible fish and shellfish from Dunedin, and other regions around the South Island, New Zealand. Mar. Pollut. Bull. 101, 386–390. https://doi.org/10.1016/j.marpolbul.2015.10.013.
Shanker, K., Mishra, S., Srivastava, S., Srivastava, R., Dass, S., Prakash, S., Srivastava, M.M., 1996. Study of mercury-selenium (Hg-Se) interactions and their impact on Hg uptake by the radish (Raphanus sativus) plant. Food Chem. Toxicol. 34, 883–886.
Singh, S.P., Vogel-Mikuš, K., Vavpetič, P., Jeromel, L., Pelicon, P., Kumar, J., Tuli, R., 2014. Spatial X-ray fluorescence micro-imaging of minerals in grain tissues of wheat and related genotypes. Planta 240, 277–289. https://doi.org/10.1007/s00425-014-2084-4.
Slejkovec, Z., van Elteren, J.T., Woroniecka, U.D., Kroon, K.J., Falnoga, I., Byrne, A.R., 2000. Preliminary study on the determination of selenium compounds in some selenium-accumulating mushrooms. Biol. Trace Elem. Res. 75, 139–155. https://doi.org/10.1385/BTER:75:1-3:139.
Slekovec, M., Goessler, W., 2005. Accumulation of selenium in natural plants and selenium supplemented vegetable and selenium speciation by HPLC-ICPMS. Chem. Speciat. Bioavailab. 17, 63–73. https://doi.org/10.3184/095422905782774919.
Spiller, H.A., 2018. Rethinking mercury: the role of selenium in the pathophysiology of mercury toxicity. Clin. Toxicol. https://doi.org/10.1080/15563650.2017.1400555.
Stijve, T., Noorloos, T., Byrne, A.R., Šlejkovec, Z., Goessler, W., 1998. High selenium levels in edible albatrellus mushrooms. Dtsch. Leb. 94, 275–279.
Thangavel, P., Sulthana, A.S., Subburam, V., 1999. Interactive effects of selenium and mercury on the restoration potential of leaves of the medicinal plant. Portulaca oleracea Linn. Sci. Total Environ. 243–244, 1–8.
Vaufleury, A.G. De, Bispo, A., 2000. Methods for toxicity assessment of contaminated soil by oral or dermal uptake in land snails. 1. Sublethal effects on growth. Environ. Sci. Technol. 34, 1865–1870. https://doi.org/10.1021/es9907212.
Vogel-Mikuš, K., Arčon, I., Kodre, A., 2010. Complexation of cadmium in seeds and vegetative tissues of the cadmium hyperaccumulator Thlaspi praecox as studied by X-ray absorption spectroscopy. Plant Soil 331, 439–451. https://doi.org/10.1007/s11104-009-0264-y.
Vogel-Mikuš, K., Pongrac, P., Pelicon, P., 2014. Micro-PIXE elemental mapping for ionome studies of crop plants. Int. J. PIXE 24, 217–233. https://doi.org/10.1142/

S0129083514400142.
Wagemann, R., Trebacz, E., Boila, G., Lockhart, W., 1998. Methylmercury and total mercury in tissues of arctic marine mammals. Sci. Total Environ. 218, 19–31. https://doi.org/10.1016/S0048-9697(98)00192-2.
White, P.J., 2016. Selenium accumulation by plants. Ann. Bot. 117, 217–235. https://doi.org/10.1093/aob/mcv180.
White, P.J., Broadley, M.R., 2009. Biofortification of crops with seven mineral elements often lacking in 49–84. https://doi.org/10.1111/j.1469-8137.2008.02738.x.
WHO/JECFA, 2007. http://apps.who.int/food-additives-contaminants-jecfa-database/chemical.aspx?chemID=3083 (accessed 6.25.19).
Xu, X., Yan, M., Liang, L., Lu, Q., Han, J., Liu, L., Feng, X., Guo, J., Wang, Y., Qiu, G., 2019. Impacts of selenium supplementation on soil mercury speciation, and inorganic mercury and methylmercury uptake in rice (Oryza sativa L.). Environ. Pollut. 249, 647–654. https://doi.org/10.1016/j.envpol.2019.03.095.
Zhang, H., Feng, X., Chan, H.M., Larssen, T., 2014. New insights into traditional health risk assessments of mercury exposure: implications of Selenium. Environ. Sci. Technol. 48, 1206–1212. https://doi.org/10.1021/es4051082.
Zhang, H., Feng, X., Zhu, J., Sapkota, A., Meng, B., Yao, H., Qin, H., Larssen, T., 2012. Selenium in soil inhibits mercury uptake and translocation in rice (Oryza sativa L.). Environ. Sci. Technol. 46, 10040–10046. https://doi.org/10.1021/es302245r.
Zhao, J., Chen, C., Zhang, P., Chai, Z., Qu, L., Li, M., 2004. Preliminary study of selenium and mercury distribution in some porcine tissues and their subcellular fractions by NAA and HG-AFS. J. Radioanal. Nucl. Chem. 259, 459–463. https://doi.org/10.1023/B:JRNC.0000020918.92350.40.
Zhao, J., Gao, Y., Li, Y.F., Hu, Y., Peng, X., Dong, Y., Li, B., Chen, C., Chai, Z., 2013. Selenium inhibits the phytotoxicity of mercury in garlic (Allium sativum). Environ. Res. 125, 75–81. https://doi.org/10.1016/j.envres.2013.01.010.
Zidar, P., Kos, M., Vogel-Mikuš, K., van Elteren, J.T., Debeljak, M., Žižek, S., 2016. Impact of ionophore monensin on performance and Cu uptake in earthworm Eisenia andrei exposed to copper-contaminated soil. Chemosphere 161, 119–126. https://doi.org/10.1016/j.chemosphere.2016.07.013.
Zwolak, I., Zaporowska, H., 2012. Selenium interactions and toxicity: a review. Cell Biol. Toxicol. https://doi.org/10.1007/s10565-011-9203-9.